6-19-2015

Detection of Small-Scale Rockfall Incidents Using Their Seismic Signature

Achilleas Tripolitsiotis
Technical University of Crete, Greece

Antonis Daskalakis
Technical University of Crete, Greece

Stelios Mertikas
Technical University of Crete, Greece

Dionysios Hristopulos
Technical University of Crete, Greece

Zacharias Agioutantis
University of Kentucky, zach.agioutantis@uky.edu

See next page for additional authors

Authors
Achilleas Tripolitsiotis, Antonis Daskalakis, Stelios Mertikas, Dionysios Hristopulos, Zacharias Agioutantis, and Panagiotis Partsinevelos

Detection of Small-Scale Rockfall Incidents Using Their Seismic Signature

Notes/Citation Information
Published in *Proceedings of SPIE*, v. 9535, 953519, p. 1-9.

Achilleas Tripolitsiotis, Antonis Daskalakis, Stelios Mertikas, Dionysios Hristopulos, Zach Agioutantis, Panagiotis Partsinevelos, "Detection of small-scale rockfall incidents using their seismic signature", 9535, Third International Conference on Remote Sensing and Geoinformation of the Environment, 953519 (June 19, 2015). DOI: https://doi.org/10.1117/12.2192591

Digital Object Identifier (DOI)
https://doi.org/10.1117/12.2192591

Detection of small-scale rockfall incidents using their seismic signature

Achilleas Tripolitsiotis*[a], Antonis Daskalakis[a], Stelios Mertikas[a], Dionysios Hristopulos[a], Zach Agioutantis[b], Panagiotis Partsinevelos[a]

[a]Technical University of Crete, School of Mineral Resources Engineering, , GR-73100 Chania, Greece, email: atripol@mred.tuc.gr.
[b]University of Kentucky, Department of Mining Engineering, Lexington, Kentucky, USA, email: zach.agioutantis@uky.edu

ABSTRACT

Several algorithms have been effectively used to identify the seismic signature of rockfall incidents, which constitute a significant threat for human lives and infrastructure especially when occurring along transportation networks. These algorithms have been mostly evaluated using data from large scale rockfall events that release a large amount of energy. However, low-energy rockfall events (< 100 Joules) triggered by small-sized individual rocks falling from small heights can be severely destructive. In this study, a three-parameter algorithm has been developed to identify low-energy rockfall events. An experimental setup was implemented to 1) validate the results obtained by this algorithm against visual inspection of seismic signals records, 2) define the optimal algorithm parameterization to minimize false alarms, and 3) investigate whether tri-axial vibration monitoring can be replaced by a uniaxial device in order to reduce the installation cost of a real-time rockfall monitoring system. It was found that the success rate of the proposed algorithm exceeds 80% independently of the parameters used, while event identification at a maximum distance with minimal false alarms was achieved when using $mean \pm 3\sigma$ as the threshold criterion and 6 ms and 4 ms as the trigger and event window parameters respectively. Finally, it was found that for the specific experimental setup, a uniaxial device could be used for rockfall event identification.

Keywords: rockfall, change detection, seismic signals

1. INTRODUCTION

Early detection of rockfall incidents along transportation routes is an important element for efficient risk management and improvement of public safety. Roads and railways passing through mountainous areas are endangered by the sudden detachment of a rock mass that may lead to stopping traffic [1], infrastructure damage and even casualties [2].

In order to estimate the potential rockfall risk along transportation corridors, several qualitative rick rating systems have been proposed and implemented mainly by transportation agencies [3]. Defensive structures such as fences, barriers embankments are commonly used in high-rick areas. However, the cost for the installation of these structures is relatively high and their installation may not be affordable in several areas. This is the reason why, several near real-time monitoring systems have been proposed to monitor large areas of interest using terrestrial remote sensors (i.e., total stations, terrestrial laser scanners, ground-based interferomertric SAR sensors) [4] and imaging techniques [5], [6].

These instruments provide precise measurements of the slope geometrical characteristics, do not provide 24/7 measurements (i.e., imaging techniques), are strongly influenced by the meteorological conditions that prevail the area of interest (i.e., total stations) or are highly expensive (i.e., ground-based InSAR). Moreover, the computational needs and processing time for the majority of these systems constitute a drawback for their incorporation into an operational rockfall monitoring system.

On the other hand, geophysical sensors (i.e., geophones, accelerometers, seismographs) are weather independent, operate in harsh environments and provide reliable, continuous, and day-and-night monitoring capabilities. Seismic signals associated with rockfalls and other mass movements have been studied extensively in many geological contexts. For

Third International Conference on Remote Sensing and Geoinformation of the Environment (RSCy2015), edited by Diofantos G. Hadjimitsis, Kyriacos Themistocleous, Silas Michaelides, Giorgos Papadavid, Proc. of SPIE Vol. 9535, 953519 · © 2015 SPIE · CCC code: 0277-786X/15/$18 · doi: 10.1117/12.2192591

example, in [7] analysis of seismic records of 14 large (> 104 m^3) rockfalls and avalanches between 1963 and 1992 was performed and the author noted that the events were detected in the seismic records. More recently, in [8] and [9] the ability of seismic signals to provide important information on the characteristics of the rockfall (e.g., volume, duration, and location) was reported. Whereas these studies focused on the analysis of large scale rockfalls, in [10] the seismic signature of small scaled (1-10 m^3) rockfall incidents that occur more frequently than large events was examined and analyzed. In [11] field experiments with the free fall of 12 kg and 50 kg stones over a channel bed and the ground vibrations caused by these falls are analyzed. In other studies, i.e. [12-15], different algorithms have been proposed and implemented in the scientific literature for the identification of the seismic signature of rockfall events.

In this work, Section 2 presents a three parameter rockfall event detection automatic methodology ("ISTRIA" algorithm) along with the description of the experimental setup established for its evaluation. Section 3 provides the results of the analysis performed and the algorithm is evaluated against the number of events identified, the number of false alarms produced and the optimum parameterization is proposed. Finally, in Section 4 recommendations for further validation of the proposed algorithm are given.

2. "ISTRIA" ALGORITHM AND EXPERIMENTAL SETUP

The quality of a rockfall event identification algorithm may be quantitatively measured with its ability to identify all events present in the seismic signal, the number of parameters necessary for its implementation, the number of false alarms generated, the computational time, etc. The first criterion is related to the overall success of the algorithm whereas the rest of the criteria should be kept as low as possible. Given that the above mentioned studies rely upon multi-parametric algorithms or high order statistics that require a considerable amount of data, a simple automated algorithm for rockfall event identification based on their seismic signature that should work with limited data availability was developed under the framework of the "ISTRIA" research proposal co-funded by the European Regional Development Fund (ERDF) and the Greek government.

The "ISTRIA" algorithm is a modified version of the moving window trigger (MWT) algorithm that was originally developed to identify and characterize low dissolved oxygen (DO) events and designed to treat time series of arbitrary sampling resolution and duration [16]. Based on the initial implementation of the MWT algorithm, the "ISTRIA" algorithm identifies rock-fall events which simultaneously produce geophone signatures that exceed certain limits (Threshold parameter) and last more than a specified time window (Event-window parameter) (see Fig.1). The "ISTRIA" algorithm was implemented in the MATLAB technical computing language and employs an overlapping window (Trigger window parameter) to search for rock-fall events within the signal.

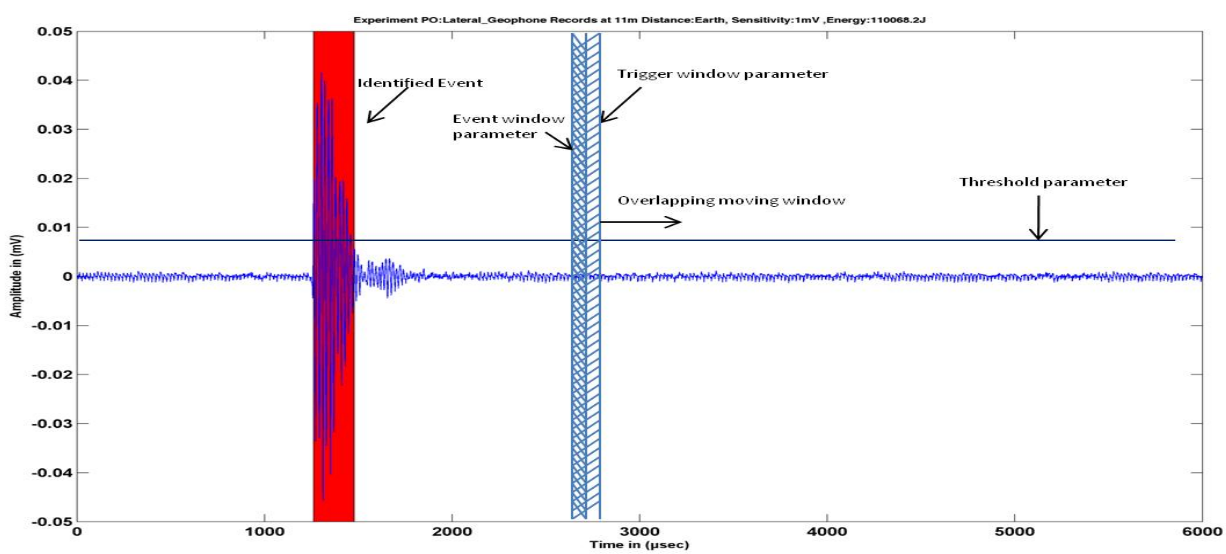

Figure 1: Schematic representation of the parameters (threshold, trigger window, event duration window) used in the "ISTRIA" algorithm.

In order to qualitatively test the performance of the algorithm an experimental setup was implemented and presented in [17]. There, the threshold value was set to mean ± 2σ, and the trigger and event duration windows to 5 ms and 3 ms respectively and it was found that a spacing of 15-30 m is adequate to capture rockfall incidents with an impact energy above 30 J.

In this work, a new experimental setup was implemented to deliver a more detailed evaluation of the performance of the proposed algorithm including its optimal parameterization. The experiment took place inside the Technical University of Crete campus in Chania, Crete, Greece and, besides the evaluation of the algorithm, it focused on whether there exists a dominant direction (X-, Y-, or Z-) that could be used to replace the more expensive triaxial monitoring devices. Eight 14 Hz horizontal component geophones along with four 4.5 Hz vertical ones and a 12channel GEODE^{TM} seismograph were used for this experiment and the geophones were grouped to permit simultaneous horizontal (lateral and longitudinal) and vertical capture of the seismic signature generated in four different distances from the source (Fig. 2). The seismograph's sensitivity was set to 1mV, the sampling rate to 0.5 ms and the recording length to 3 s leading to 6000 samples per drop. A 6.73 kg concrete sphere was dropped (free fall) from a 1.65 m height resulting in a released energy of 108.93 J.

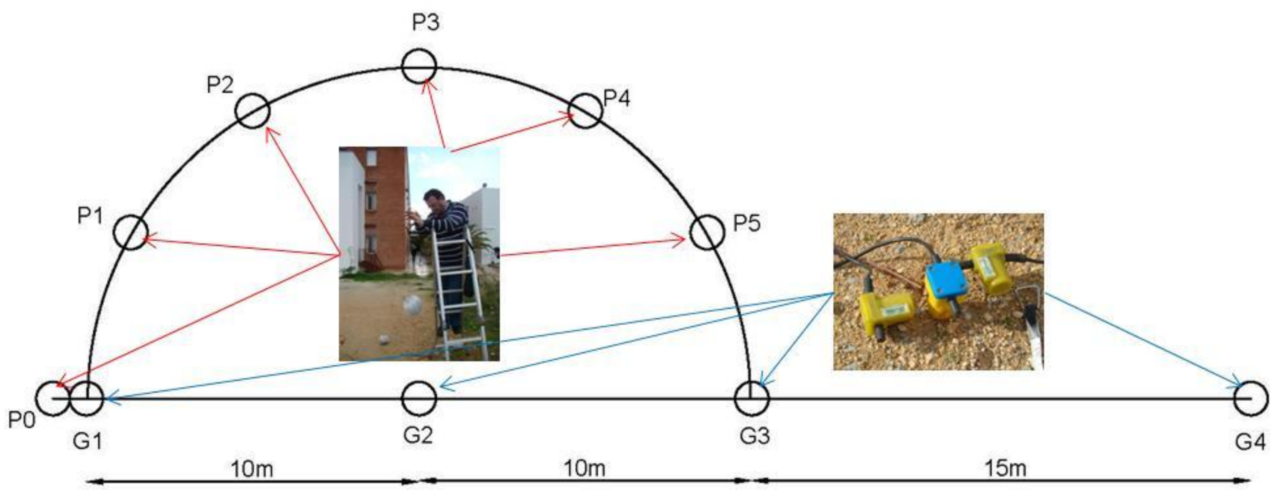

Figure 2: The experimental setup layout. Four groups of geophones (G_i) each one with two horizontal and one vertical geophone were used to capture seismic signature generated by the free fall of a 6.73 kg concrete sphere from 1.65 m height at locations P_i.

In each location P_i, three successive drops were made to ensure repeatability and better evaluation of the algorithm's performance (Table 1). Analysis of these seismic records are provided in the following Section.

Table 1: The seismic records per drop location.

Location	1st fall (Exp. No.)	2nd Fall (Exp. No.)	3rd fall (Exp. No.)
P0	1000	1001	1002
P1	1100	1101	1102
P2	1200	1201	1202
P3	1300	1301	1302
P4	1400	1401	1402
P5	1500	1501	1502

3. EXPERIMENTAL RESULTS ANALYSIS

The main objective of this work is to identify the optimal parameterization of the proposed algorithm for rockfall event detection based on their seismic signature. To accomplish this, the algorithm was applied in the seismic records (Table 1) setting the following parameter values: Trigger window (ms): 4/5/6, Event window: 2/3/4, Threshold: mean ± 2 std/ mean ± 3 std. For each seismic record, there are 18 unique combinations of the parameters values for each direction (lateral, longitudinal or vertical) thus almost 1000 records (= 18 records × 18 combinations × 3 directions) were inspected to evaluate the algorithm's performance.

In Fig. 3 a series of the G3 longitudinal records (amplitude vs time) for experiment No. 1201, for every possible combination is provided.

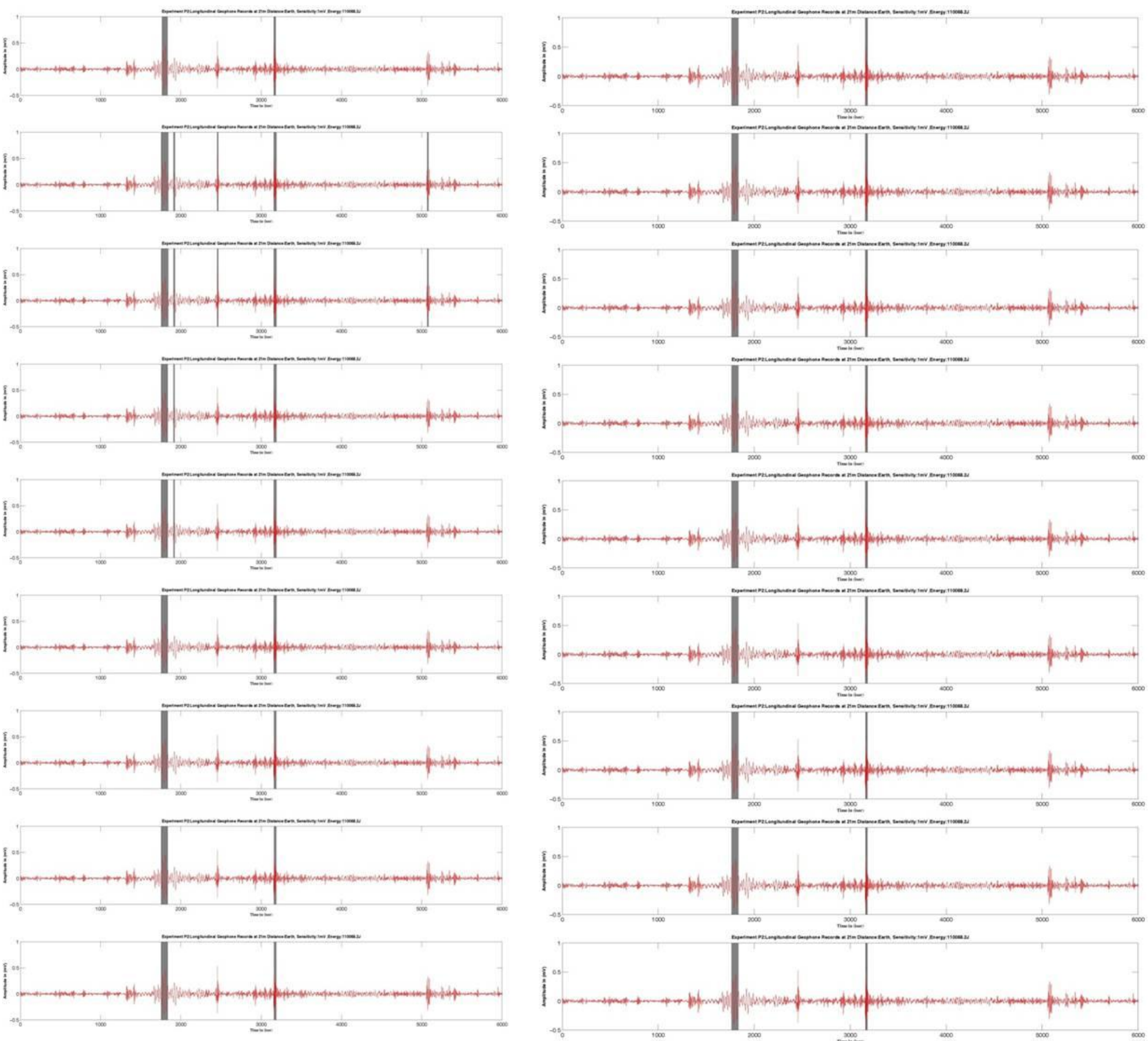

Figure 3: The seismograms produced for experiment No. 1201(location of drop: P2) after applying the proposed algorithm in the records for longitudinal geophone in the G3 geophone group. The left column presents the seismograms when the threshold is set to mean ± 2σ whereas the right column corresponds to mean ± 3σ threshold. In each column the following combinations for trigger and event duration parameters are presented: [4,2], [4,3], [4,4], [5,2], [5,3], [5,4], [6,2], [6,3], [6,4] in ms.

The grey sections in each seismogram illustrate the result of the implementation of the algorithm, and correspond to when an event has been detected. The time of the event occurrence was then compared to the one reported on site and corresponds to the time when the concrete sphere reached the ground.

The analysis revealed that changes in the algorithm's parameters influenced its ability to capture the real event, irrespectively the direction used. For example, in experiment No. 1301 and for the same trigger (5 ms) and event duration (3 ms) windows, the change of the threshold from mean ± 2σ to mean ± 3σ did not yield to event identification in the G1 vertical geophone records. However, when the trigger window was set to 4 ms and the rest of the parameters remained the same (event duration: 2 ms and threshold: mean ± 3σ) it was found that the event was clearly captured by the proposed algorithm.

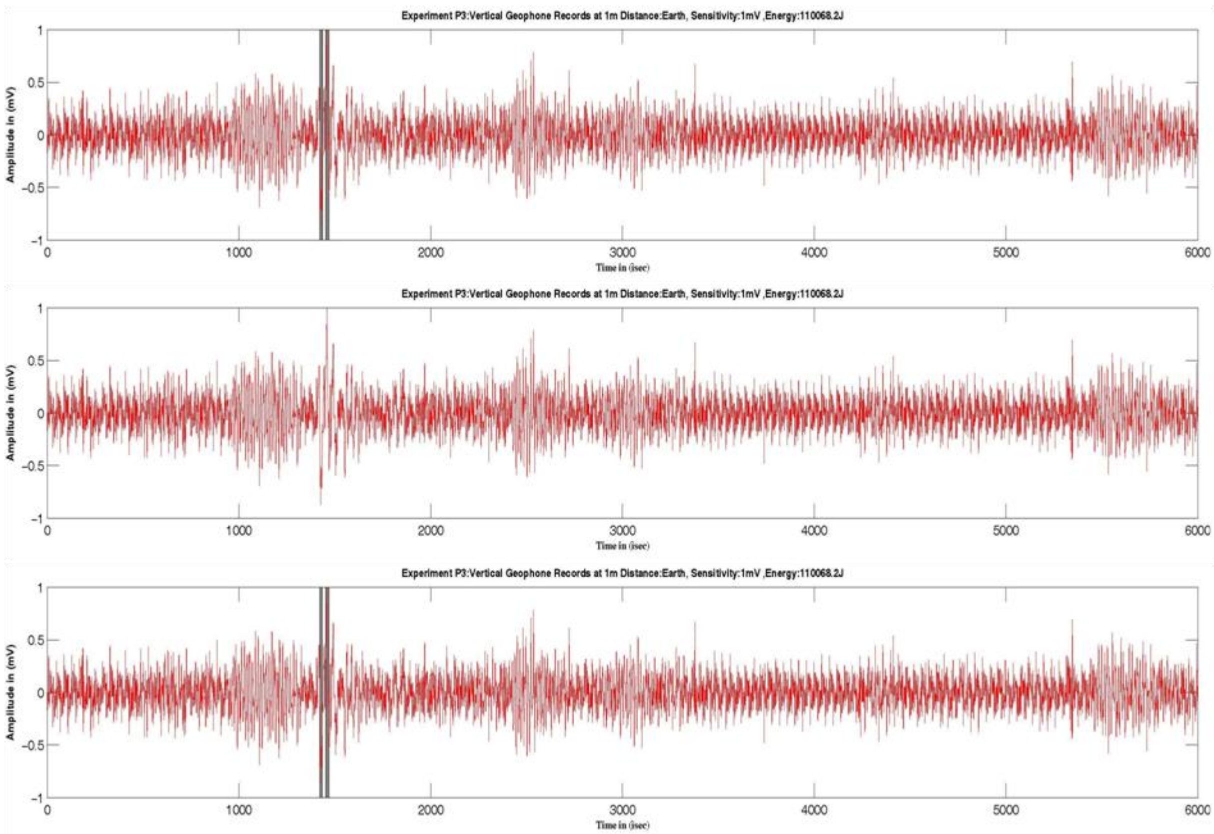

Figure 4: The effect of parameterization [trigger, event, threshold] in the algorithm's ability to capture rockfall events. In the upper image and using [5, 2, mean ± 2σ] values the algorithm captured the event whereas when using [5, 2, mean ± 3σ] the event could not be captured (middle image). Finally, usage of [4, 2, mean ± 3σ] permitted event identification.

Analysis of all records revealed that the threshold is the parameter that when changed affects mostly the algorithm's performance in event detection. Table 2 presents the success rate of the proposed algorithm that is the percentage of real events automatic identification in each direction and for all parameter combinations.

Table 2: The proposed MWT algorithm success rate in event identification.

	Success rate (%)		
Distance range (m)	**Lateral**	**Longitudinal**	**Vertical**
0-10m	100.00	100.00	96.11
10-20m	95.60	96.99	89.58
20-30m	100.00	100.00	100.00
30-40m	78.40	100.00	100.00

Another quantitative criterion that was examined to evaluate the performance of the algorithm is the number of false alarms produced per parameter and per direction. This is an important criterion especially when an algorithm is going to be incorporated into an operational early warning system. For every location (P_i) the average number of false alarms generated for the three successive drops of the concrete sphere and for each direction was calculated. Table 3 presents the impact that the threshold parameter has in the overall number of false alarms.

Table 3: Impact of threshold parameter change in the number of false alarm produced. Each number corresponds to the average of the three experiments performed in every location P_i.

	Mean ± 2σ			**Mean** ± 3σ			**Reduction (%)**		
	Lateral	Longitudinal	Vertical	Lateral	Longitudinal	Vertical	Lateral	Longitudinal	Vertical
P_0	0.78	1.17	0.70	0.44	0.42	0.03	44.25	63.69	95.05
P_1	0.32	1.02	0.74	0.06	0.31	0.17	80.43	70.07	76.64
P_2	0.81	1.20	0.23	0.38	0.58	0.02	53.45	51.45	90.91
P_3	1.57	1.30	0.52	0.83	0.76	0.08	46.90	41.18	84.00
P_4	1.38	1.47	1.58	0.35	0.44	0.30	74.87	69.67	81.14
P_5	0.69	1.26	1.63	0.32	0.40	0.40	53.54	68.13	75.32

The selection of the optimal combination between the trigger and event window duration in terms of the number of false alarms generated, was made through analysis of data provided in Table 4. It can be safely extracted that, for all directions, the minimal number of false alarms is observed when the trigger window is set to 6 ms and then that the influence of the event duration window is negligible.

Table 4: Average false alarms per drop location, direction and every possible combination of trigger and event window parameters.

Threshold: Mean ± 3σ, Trigger Window: 4ms									
Direction:	Lateral			Longitudinal			Vertical		
Drop/Event	2ms	3ms	4ms	2ms	3ms	4ms	2ms	3ms	4ms
P_0	0.56	0.56	0.50	0.56	0.56	0.44	0.19	0.13	0.00
P_1	0.06	0.06	0.06	0.56	0.38	0.50	0.19	0.19	0.19
P_2	0.38	0.38	0.38	0.81	0.75	0.50	0.06	0.00	0.00
P_3	1.19	1.06	0.94	1.13	0.81	0.81	0.19	0.13	0.06
P_4	0.56	0.31	0.25	0.56	0.75	0.56	0.56	0.50	0.44
P_5	0.44	0.44	0.38	0.56	0.50	0.50	0.56	0.56	0.38
Average	0.53	0.47	0.42	0.70	0.63	0.55	0.29	0.25	0.18
Threshold: Mean ± 3σ, Trigger Window: 5ms									
P_0	0.44	0.38	0.38	0.44	0.44	0.44	0.00	0.00	0.00
P_1	0.06	0.06	0.06	0.19	0.19	0.19	0.19	0.19	0.19
P_2	0.38	0.38	0.38	0.56	0.56	0.50	0.00	0.00	0.00
P_3	0.81	0.81	0.81	0.75	0.75	0.75	0.06	0.06	0.06
P_4	0.31	0.25	0.50	0.44	0.38	0.38	0.31	0.25	0.06
P_5	0.31	0.38	0.25	0.38	0.38	0.38	0.50	0.44	0.44
Average	0.39	0.38	0.40	0.46	0.45	0.44	0.18	0.16	0.13
Threshold: Mean ± 3σ, Trigger Window: 6ms									
P_0	0.38	0.38	0.38	0.31	0.31	0.31	0.00	0.00	0.00
P_1	0.06	0.06	0.06	0.25	0.25	0.25	0.19	0.13	0.13
P_2	0.38	0.38	0.38	0.56	0.50	0.50	0.00	0.00	0.13
P_3	0.63	0.63	0.63	0.69	0.63	0.56	0.06	0.06	0.06
P_4	0.31	0.44	0.19	0.31	0.31	0.31	0.19	0.19	0.19
P_5	0.25	0.25	0.19	0.31	0.31	0.31	0.25	0.25	0.25
Average	0.33	0.35	0.30	0.41	0.39	0.38	0.11	0.10	0.13

Moreover, it is apparent that the trigger and event windows impact on the number of false alarms depends also by the geophone orientation and that the vertical direction presents the minimal number of false alarms (Fig. 5).

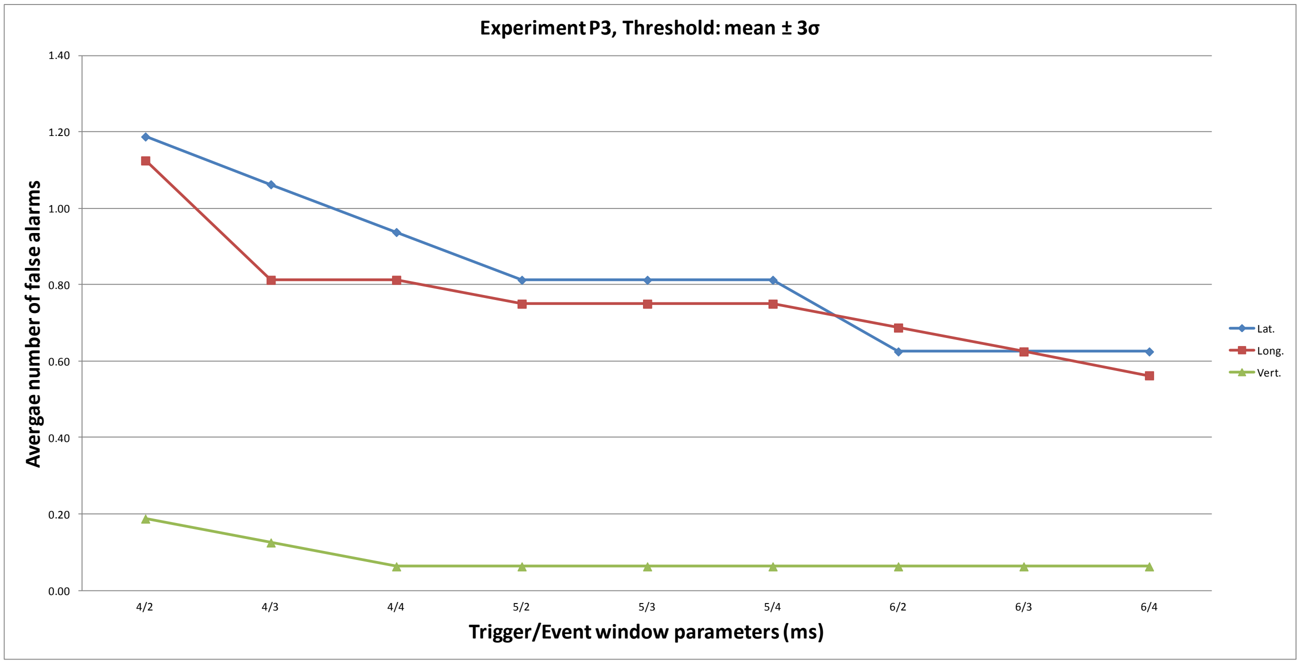

Figure 5: The relation between the average number of false alarms (Y-axis) and the trigger and event windows combinations (X-axis) for experiment P3, threshold equal to mean ± 3σ, and for the three directions: lateral (blue), longitudinal (red), and vertical (green). It is evident that the vertical direction produce the minimal number of false alarms.

4. CONCLUSIONS

A rockfall event occurs when moving rocks lose their contact with the slope. Depending on the number and the size of the rock, the area where this movement is ceased, the rockfall incident may be inconsequential with minor impact or can even be characterized as a natural disaster affecting human lives and property loses. The main objective of the experimental setup presented in this work was to propose a three parameter, automatic methodology to be used to capture rockfall incidents using their seismic signature. The experimental setup was designed to address small-scale rockfall events that have not been studied extensively so far. The main findings of this work are:

- the proposed algorithm require only three parameters (threshold, trigger window, event duration window);
- the algorithm has over 80% success rate in event identification for all experiments conducted;
- a rockfall that releases 100 J of energy produces seismic signal that can be captured by the "ISTRIA" algorithm from a geophone placed 36m away independently on the parameters used;
- the algorithm's performance in terms of false alarms generation is highly related to the threshold criterion and it was found that when the value was set to *mean* ± *3σ* the number of false alarms produced reduced by 40 - 95%;
- the trigger window parameter influence the number of false alarms and it was found that optimal results are extracted when using 6 ms as input;
- the event duration window has negligible impact on false alarm generation with slightly better results obtained when the parameter is set to 4 ms;
- the vertical direction seems to present the optimal results in terms of event identification and minimal false alarm generation.

Future work involves the execution of manually induced rockfall incidents to verify the above mentioned results under real conditions. Moreover, comparison of the algorithm's performance against well-established but poly-parametric algorithms and the optimal geophone spacing for reliable rockfall event detection are to be implemented.

ACKNOWLEDGMENTS

This work has been performed under the framework of the “Cooperation 2011” project ISTRIA (11_SYN_9_1389) funded from the Operational Program “Competitiveness and Entrepreneurship” (co-funded by the European Regional Development Fund (ERDF)) and managed by the Greek General Secretariat for Research and Technology.

REFERENCES

[1] BBC, "Rock fall closes Gret Orme road at LIandundo", July 24 2014, <http://www.bbc.com/news/uk-wales-north-west-wales-28469099>, (17 Aug 2014).

[2] Jones, G., “Falling rock derails train in French Alps, two dead” Reuters, Feb 8 2014, <http://uk.reuters.com/article/2014/02/08/uk-france-train-crash-idUKBREA170D720140208>, (04 March 2014).

[3] Budetta, P and Nappi, M., "Comparison between qualitative rockfall rick rating systems for a road affected by high traffic intensity", Nat. Haz. Earth Syst. Sci, 13, 1643-1653, 2013.

[4] Arosio, D., Longoni, L., Papini, M., Scaioni, M., Zanzi, I., Alba, M., "Towards rockfall forecasting through observing deformation and listening to microseismic emissions", Nat. Haz. Earth Syst. Sci, 9, 1119-1131, (2009).

[5] Curtaz, M., Ferrero, A.M., Roncella, R., Segalini, A., Umili, G., "Terrestrial photogrammetry and numerical modeling for the stability analysis of rock slopes in high mountain areas: Aiguilles Marbrees case", Rock Mechanics and Rock Engineering, 47, 605-620, (2014).

[6] Partsinevelos, P., Mertikas S., Agioutantis, Z., Tsioukas, V., Tripolitsiotis, A., Zervos, P., "Rockfall detection along road networks using close range photogrammetry", Proc. SPIE 9229, Second International Conference on Remote Sensing and Geoinformation of the Environment (RSCy2014), 92291M, (2014).

[7] Norris R. D., "Seismicity of rockfalls and avalanches at three Cascade Range volcanoes: implications for seismic detection of hazardous mass movements", Bull. Seis. Soc. Am., 84, 1925-1939, (1994).

[8] Hibert, C., Mangency, A., Grandjean, G., Shapiro M. N., "Slope instabilities in Dolomieu crater, Reunion Island: From seismic signals to rockfall characteristics", J. Geophys. Res., 116, F04032, (2011).

[9] Deparis, J., Jongmans, D., Cotton, F., Bailet, L., Thouvenot, F., Hantz, D., "Analysis of rock-fall and rock-fall avalanche seismograms in the French Alps", Bull. Seismol. Soc. Am., 98(4), 1781-1796, (2008).

[10] Vilajosana, I., Surinach, E., Abellan, A., Khazaradze, G., Garcia, D., Llosa, J., "Rockfall induced seismic signals: case study in Montserrat, Catalonia", Nat. Haz. Earth Syst. Sci, 8, 805-812, (2008).

[11] Huang, C.J., Yin, H.Y., Chen, C.Y., "Ground vibration produced by rock motions and debris flows", J. Geophys Res., 112, F02014, (2007).

[12] DeRoin, N. and McNutt, R.S., "Rockfalls at Augustine Volcano, Alaska: The influence of eruption precursors and seasonal factors on occurrence patterns 1997-2009", Journal of Volcanology and Geothermal Research, 211-212, 61-75, (2012).

[13] Helmstetter, A. and Garambois, S., "Seismic monitoring of Sechilienne Rockslide (French Alps): analysis of seismic signals and their correlation with rainfalls", J. Geophys. Res., 115 (F3), F03016, (2010).

[14] Dammeier, F., Moore, J. R., Haslinger F., Loew, S., "Characterization of alpine rockslides using statistical analysis of seismic signals", J. Geophys. Res., 116, F04024, doi:10.1029/2011JF002037, (2011).

[15] Hibert, C., Mangeney, A., Grandjean, G., Bailard, C., Rivet, D., Shapiro, N.M., Satriano, C., Maggi, A., Boisser, P., Ferrazzini, V., Crawford, W., "Automated identification, location, and volume estimation of rockfalls at Piton de la Fournaise volcano", Journal of Geophysical Research: Earth Surface, Vol. 119 (5), pp 1082-1105, (2014).

[16] Codiga, D.L., Stoffel, H. E., Deacutis, C.F, Kiernan, S., Oviatt, C.A., "Narragansett Bay Hypoxic Event Characteristics Based on Fixed-Site Monitoring Network Time Series: Intermittency, Geographic Distribution, Spatial Synchronicity, and Interannual Variability", Estuaries and Coasts, 32(4), pp 621-641, (2009).

[17] Agioutantis Z., Mertikas, S., Steiakakis, C., Daskalakis, A., Tripolitsiotis, A., Krtitikakis, G., Apostolou, E., Kaplanidis, G., "Rockfall monitoring system for improving road safety", The 2014 ISRM European Rock Mechanics Symposium-EUROCK2014, Vigo, Spain, 27-29th May 2014, (2014).